

AN ITERATIVE TECHNIQUE TO COMPENSATE FOR POSITIONING ERRORS IN THE NF-FF TRANSFORMATION WITH HELICOIDAL SCANNING FOR LONG ANTENNAS

**F. D'Agostino, F. Ferrara, C. Gennarelli, R. Guerriero
and M. Migliozzi**

Dipartimento di Ingegneria dell'Informazione ed Ingegneria Elettrica
University of Salerno
via Ponte Don Melillo, Fisciano (Salerno) 84084, Italy

Abstract—An effective procedure is developed in this paper to compensate the probe positioning errors when using a near-field to far-field transformation technique with helicoidal scanning for long antennas. It is based on a prolate ellipsoidal modelling of the antenna under test and makes use of an iterative scheme to retrieve the uniformly distributed helicoidal near-field data from the irregularly spaced acquired ones. Once these data have been recovered, those required to perform a standard near-field-far-field transformation with cylindrical scanning are efficiently determined via an optimal sampling interpolation algorithm. Some numerical tests are reported to assess the accuracy of the approach and its robustness with respect to random errors affecting the data. At last, the validity of the developed technique is further confirmed by the experimental tests performed at the Antenna Characterization Lab of the University of Salerno.

1. INTRODUCTION

In the last years, the antenna measurement community has spent many efforts to reduce the time needed for the acquisition of the near-field data, since such a time is currently very much greater than that required to perform the near-field-far-field (NF-FF) transformation. In the NF measurement facilities using mechanical scans, which are generally more flexible than those employing the fast electronic

ones [1], the measurement time can be reduced by using continuous and synchronized movements of the positioning systems of the probe and antenna under test (AUT) [2]. Accordingly, NF-FF transformations employing innovative spiral scanings have been recently proposed [3–12]. They rely on the nonredundant sampling representations of electromagnetic (EM) fields [13] and exploit the optimal sampling interpolation (OSI) expansions to recover the NF data needed by the NF-FF transformation with the corresponding traditional scanning. Besides the employ of continuous movements, the drastic time saving characterizing them is due to the significantly reduced number of required NF data. The OSI expansion has been obtained: a) by assuming the AUT enclosed in a proper convex domain bounded by a surface Σ with rotational symmetry; b) by developing a non-redundant sampling representation of the voltage acquired by the probe on the spiral; c) by choosing the spiral step equal to the sample spacing required to interpolate the NF data along a meridian curve. In particular, the AUT has been considered as enclosed in the smallest sphere able to contain it in [3–6], whereas more effective AUT modellings, that allow a further reduction of the required NF data in the case of elongated or quasi-planar antennas, have been adopted in [7–11] by properly employing the unified theory of spiral scans for nonspherical antennas [12]. These modellings allow one to consider measurement cylinders (planes) with a radius (distance) smaller than one half the AUT maximum size, thus reducing the error related to the truncation of the scanning zone.

In the practice, the errors due to an inaccurate control of the positioning systems do not allow one to obtain regularly spaced NF measurements, even though their position can be precisely read by optical tools. Moreover, the finite resolution of the positioning devices, as well as, their inaccurate synchronization prevent the possibility to exactly locate the receiving probe at the points specified by the sampling representation. Accordingly, the development of an accurate and stable reconstruction algorithm from irregularly distributed data becomes meaningful.

An approach based on the conjugate gradient iteration method and using the unequally spaced fast Fourier transform [14, 15] has been proposed in the planar [16] and spherical [17] classical scanings. In any case, such an approach is not suitable for scanning techniques taking advantage of the nonredundant sampling representations of EM fields, wherein the “a priori” information on the AUT and proper OSI formulas are employed to reconstruct the NF data required by the corresponding standard NF-FF transformation. As stressed in [18] wherein a more detailed discussion can be found, the formulas available

in literature for the direct reconstruction from nonuniform samples are valid only for particular sampling points distributions, are not user friendly, and become more and more unstable as the sampling points arrangement deviates from the uniform one. A viable and convenient strategy is to retrieve the uniform samples from those irregularly spaced and then determine the value at any point of the scanning surface by an accurate and stable OSI formula. Two approaches [18–20] have been proposed to this end and compared and experimentally validated in [21]. The former [18,19] is based on an iterative technique which is resulted to be convergent only if there exists a one-to-one correspondence associating at each uniform sampling point the nearest nonuniform one. The latter [20] makes use of the singular value decomposition (SVD) method and has been applied when the two-dimensional problem can be tackled as two independent one-dimensional ones. This occurs, e.g., in the cylindrical scanning, wherein the non-uniform samples can be assumed to lie on not regularly spaced rings [21].

This last hypothesis is not valid in the helicoidal scanning case and, as a consequence, the iterative technique is applied in the following to recover the uniformly distributed helicoidal samples from the irregularly spaced collected ones, whose position is assumed known since it can be determined, f.i., by using a laser tracker. In particular, the helicoidal scanning technique [7] tailored for electrically long antennas and using a prolate ellipsoidal AUT modelling is considered. Obviously, the SVD-based approach could be generalized to such a two-dimensional problem, but the dimension of the involved matrix would become very large, thus requiring a massive computational effort. The effectiveness of the iterative scheme for compensating the positioning errors in the corresponding NF-FF transformation will be here validated both by numerical simulations and laboratory tests performed at the UNISA Antenna Characterization Lab.

2. VOLTAGE REPRESENTATION ON A CYLINDER FROM UNIFORM HELICOIDAL SAMPLES

Let us consider an elongated AUT enclosed in a prolate ellipsoid Σ having major and minor semiaxes equal to a and b and a nondirective probe scanning a proper helix lying on a cylinder of radius d (Fig. 1). The spherical coordinate system (r, ϑ, φ) is adopted to denote an observation point P both in the NF and FF region. Since the voltage V measured by such a probe has the same effective spatial bandwidth of the field, the nonredundant representations of EM fields [13] can be applied to it. Accordingly, when dealing with the representation on a

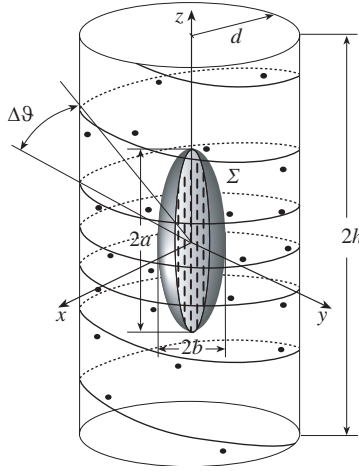


Figure 1. Geometry of the problem.

curve C , it is convenient to adopt a proper analytical parameterization $\underline{r} = \underline{r}(\eta)$ to describe C and to introduce the “reduced voltage”

$$\tilde{V}(\eta) = V(\eta)e^{j\psi(\eta)} \quad (1)$$

where $\psi(\eta)$ is a proper phase function. The error, occurring when $\tilde{V}(\eta)$ is approximated by a bandlimited function, becomes negligible as the bandwidth exceeds a critical value W_η [13], so that it can be effectively controlled by choosing a bandwidth equal to $\chi'W_\eta$, χ' being an excess bandwidth factor slightly greater than unity for a large AUT.

As shown in [7], a two-dimensional OSI algorithm to reconstruct the voltage from a nonredundant number of its samples collected by the probe along a helix can be obtained by developing a nonredundant sampling representation of the voltage on a helix, whose step must be chosen equal to the sample spacing required to interpolate the data along a generatrix. In particular, the bandwidth W_η and parameterization η relevant to a generatrix, and the corresponding phase function ψ are [7]:

$$W_\eta = (4a/\lambda)E(\pi/2|\varepsilon^2); \quad \eta = (\pi/2)[1 + E(\sin^{-1}u|\varepsilon^2)/E(\pi/2|\varepsilon^2)] \quad (2)$$

$$\psi = \beta a \left[v \sqrt{\frac{v^2 - 1}{v^2 - \varepsilon^2}} - E \left(\cos^{-1} \sqrt{\frac{1 - \varepsilon^2}{v^2 - \varepsilon^2}} \mid \varepsilon^2 \right) \right] \quad (3)$$

where β is the wavenumber, λ is the wavelength, $u = (r_1 - r_2)/2f$ and $v = (r_1 + r_2)/2a$ are the elliptic coordinates, $r_{1,2}$ being the distances from observation point P to the foci of C' (intersection curve between

a meridian plane and Σ) and $2f$ its focal distance. Moreover, $\varepsilon = f/a$ is the eccentricity of C' and $E(\cdot|\cdot)$ denotes the elliptic integral of second kind. It is worth noting that in any meridian plane the curves $\psi = \text{const}$ and $\eta = \text{const}$ are ellipses and hyperbolas confocal to C' , instead of circumferences and radial lines, as in the spherical modelling case. The parametric equations of the helix, obtained as projection of a proper spiral wrapping the ellipsoid Σ modelling the AUT on the scanning cylinder by means of the curves at $\eta = \text{const}$ [11] and imposing its passage through a fixed point P_0 of the generatrix at $\varphi = 0$, are:

$$\begin{cases} x = d\cos(\phi - \phi_s) \\ y = d\sin(\phi - \phi_s) \\ z = d \cot[\vartheta(\eta)] \end{cases} \quad (4)$$

wherein ϕ is the angular parameter describing the helix, ϕ_s is the value of ϕ at P_0 , and $\eta = k\phi$. The parameter k is such that the spiral step, fixed by two consecutive intersections with a generatrix, is equal to the sample spacing $\Delta\eta = 2\pi/(2N'' + 1)$ needed for the interpolation along a generatrix, where $N'' = \text{Int}(\chi N') + 1$ and $N' = \text{Int}(\chi' W_\eta) + 1$. Accordingly, being $\Delta\eta = 2\pi k$, it follows that $k = 1/(2N'' + 1)$. The function $\text{Int}(x)$ gives the integer part of x and $\chi > 1$ is an oversampling factor controlling the truncation error.

According to [12], a nonredundant representation of the probe voltage along the helix is then obtained by enforcing the parameterization ξ equal to β/W_ξ times the arclength of the projecting point on the spiral wrapping Σ and the phase function γ coincident with that ψ relevant to a generatrix. Moreover, W_ξ is chosen equal to β/π times the length of the spiral wrapping the ellipsoid from pole to pole [7].

According to these results, the voltage at any point of the helix can be reconstructed [7] by means of the OSI expansion:

$$\tilde{V}(\xi) = \sum_{m=m_0-p+1}^{m_0+p} \tilde{V}(\xi_m) G(\xi, \xi_m, M, M'') \quad (5)$$

where $m_0 = \text{Int}[(\xi - \xi_s)/\Delta\xi]$ is the index of the sample nearest (on the left) to the output point, $2p$ is the number of retained samples $\tilde{V}(\xi_m)$, and

$$\xi_m = \xi(\phi_s) + m\Delta\xi = \xi_s + 2\pi m/(2M'' + 1) \quad (6)$$

with $M'' = \text{Int}(\chi M') + 1$ and $M' = \text{Int}(\chi' W_\xi) + 1$. Moreover,

$$G(\xi, \xi_m, M, M'') = \Omega_M(\xi - \xi_m) D_{M''}(\xi - \xi_m) \quad (7)$$

wherein

$$D_{M''}(\xi) = \frac{\sin((2M'' + 1)\xi/2)}{(2M'' + 1)\sin(\xi/2)},$$

$$\Omega_M(\xi) = \frac{T_M \left[-1 + 2 \left(\cos(\xi/2) / \cos(\bar{\xi}/2) \right)^2 \right]}{T_M \left[-1 + 2 / \cos^2(\bar{\xi}/2) \right]} \quad (8)$$

are the Dirichlet and Tschebyscheff sampling functions, $T_M(\xi)$ being the Tschebyscheff polynomial of degree $M = M'' - M'$ and $\bar{\xi} = p\Delta\xi$.

The OSI formula (5) can be used to evaluate the “intermediate samples”, i.e., the voltage values at the intersection points between the helix and the generatrix through P . Once these samples have been got, the voltage at P can be determined via a quite similar OSI formula [7]. The following two-dimensional OSI expansion thus results:

$$\tilde{V}(\eta(\vartheta), \varphi) = \sum_{n=n_0-q+1}^{n_0+q} \left[G(\eta, \eta_n, N, N'') \sum_{m=m_0-p+1}^{m_0+p} \tilde{V}(\xi_m) G(\xi(\eta_n), \xi_m, M, M'') \right] \quad (9)$$

where $2q$ is the number of the retained intermediate samples, $n_0 = \text{Int}[(\eta - \eta_0)/\Delta\eta]$, $N = N'' - N'$,

$$\eta_n = \eta_n(\varphi) = \eta(\phi_s) + k\varphi + n\Delta\eta = \eta_0 + n\Delta\eta \quad (10)$$

and the other symbols have the same or analogous meaning as in (5). Expansion (9) can be employed to evaluate the voltage at any point P on the cylinder and, in particular, at those required to carry out the standard NF-FF transformation technique with cylindrical scanning [22].

3. RECONSTRUCTION OF THE UNIFORM SAMPLES

Let us now turn to the case of nonuniformly distributed samples (Fig. 1) and denote with $(\bar{\eta}_i, \bar{\varphi}_i)$ the position, assumed known, of the nonuniform sampling point corresponding to the nearest uniform one ξ_i on the helix. By expressing the reduced voltage at each nonuniform sampling point in terms of the unknown values at the nearest uniform ones via the two-dimensional OSI expansion (9) and neglecting the

truncation error, it results:

$$\tilde{V}(\bar{\eta}_i, \bar{\varphi}_i) = \sum_{n=n_0-q+1}^{n_0+q} \left[G(\bar{\eta}_i, \eta_n, N, N'') \sum_{m=m_0-p+1}^{m_0+p} \tilde{V}(\xi_m) G(\xi(\eta_n), \xi_m, M, M'') \right] \quad i=1, 2, \dots, Q \quad (11)$$

where Q is the number of sampling points. Such a linear system can be rewritten in the matrix form

$$\underline{A} \underline{x} = \underline{b} \quad (12)$$

where \underline{A} is the $Q \times Q$ sparse banded matrix whose elements are given by

$$A_{im} = G(\bar{\eta}_i, \eta_n, N, N'') G(\xi(\eta_n), \xi_m, M, M'')$$

\underline{x} is the vector of the unknown uniform samples, and \underline{b} is the vector of the acquired irregularly distributed ones.

By splitting \underline{A} into its diagonal and nondiagonal parts, \underline{A}_D and $\underline{\Delta}$ respectively, it results

$$\left(\underline{A}_D + \underline{\Delta} \right) \underline{x} = \underline{b} \quad (13)$$

multiplying both members of the system (13) by \underline{A}_D^{-1} and rearranging the terms, we get

$$\underline{x} = \underline{A}_D^{-1} \underline{b} - \underline{A}_D^{-1} \underline{\Delta} \underline{x}$$

The following iterative procedure thus results

$$\underline{x}^{(\nu)} = \underline{A}_D^{-1} \underline{b} - \underline{A}_D^{-1} \underline{\Delta} \underline{x}^{(\nu-1)} = \underline{x}^{(0)} - \underline{A}_D^{-1} \underline{\Delta} \underline{x}^{(\nu-1)} \quad (14)$$

where $\underline{x}^{(\nu)}$ is the vector of the uniform samples estimated at the ν th step. Necessary conditions for the convergence of such an algorithm [18, 19] are that $A_{ii} \neq 0, \forall i$, and $|A_{ii}| \geq |A_{im}|, \forall m \neq i$. These conditions are certainly satisfied in the here assumed hypothesis of biunique correspondence between each uniform sampling point and the “nearest” nonuniform one. By straightforward evaluations, it finally results:

$$\tilde{V}^{(\nu)}(\xi_i) = \frac{1}{A_{ii}} \left\{ \tilde{V}(\bar{\eta}_i, \bar{\varphi}_i) - \sum_{n=n_0-q+1}^{n_0+q} \left[G(\bar{\eta}_i, \eta_n, N, N'') \sum_{\substack{m=m_0-p+1 \\ m \neq i}}^{m_0+p} \tilde{V}^{(\nu-1)}(\xi_m) G(\xi(\eta_n), \xi_m, M, M'') \right] \right\} \quad (15)$$

wherein

$$A_{ii} = G(\bar{\eta}_i, \eta_{n_i}, N, N'') G(\xi(\eta_{n_i}), \xi_i, M, M'') \quad (16)$$

$n_i = \text{Nint}[(\bar{\eta}_i - \eta_0)/\Delta\eta]$ being the index of the intermediate sampling point nearest to the uniform one ξ_i .

4. NUMERICAL AND EXPERIMENTAL VALIDATION

In this section, the effectiveness of the proposed iterative scheme for compensating the positioning errors in the NF-FF transformation with helicoidal scanning is validated both by numerical simulations and laboratory tests.

The numerical tests refer to a helix lying on a cylinder with radius $d = 12\lambda$ and height $2h = 180\lambda$. The AUT is a uniform planar array located in the plane $y = 0$, whose elements are elementary Huygens sources polarized along the z axis. They are spaced by 0.7λ and cover an elliptical zone with semi-axes equal to 30λ and 6λ , so that the antenna can be very well fitted by a prolate ellipsoid. An open-ended WR-90 rectangular waveguide at the frequency of 10 GHz is chosen as probe. The nonuniform samples have been generated by imposing that the distances in ξ and η between the position of each nonuniform sample and the associate uniform one are random variables uniformly distributed in $(-0.3\Delta\xi, 0.3\Delta\xi)$ and $(-0.3\Delta\eta, 0.3\Delta\eta)$, which represents a pessimistic occurrence in a real scanning procedure.

Figures 2 and 3 show a reconstruction example of the voltage V (the most significant one) on the generatrix at $\varphi = 90^\circ$, obtained by 0 and 6 iterations, respectively. As it can be seen, only 6 iterations are enough to achieve a very good agreement between the exact curve and the reconstructed one. The algorithm performances have been assessed by evaluating the mean-square errors in the reconstruction of the uniform samples. These errors (see Fig. 4) are normalized to the voltage maximum value on the scan cylinder and have been obtained by comparing the reconstructed uniform samples and the exact ones in the central zone of the scanning surface, thus assuring the existence of the guard samples. As it can be seen, the errors, on increasing the number of iterations, decrease quickly until a constant saturation value is reached. Such a value decreases on increasing the retained samples number. Even better results are to be expected when the nonuniform samples are closer to the uniform ones. The errors curves can be employed as an effective aid to choose, for a given accuracy, the proper values of parameters to be used in (15) as well as to fix the number of needed iterations.

The algorithm robustness has been assessed (see Fig. 5) by adding random errors to the exact samples. These errors simulate a background noise (bounded to Δa dB in amplitude and with arbitrary phase) and an uncertainty on the data of $\pm\Delta a_r$ dB in amplitude and $\pm\Delta\alpha$ degrees in phase.

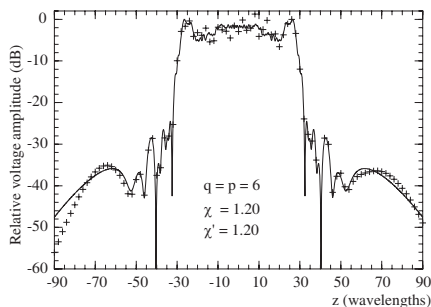


Figure 2. Amplitude of the probe voltage on the generatrix at $\varphi = 90^\circ$. Solid line: exact. Crosses: recovered from irregularly spaced NF helicoidal data via the iterative technique using zero iterations.

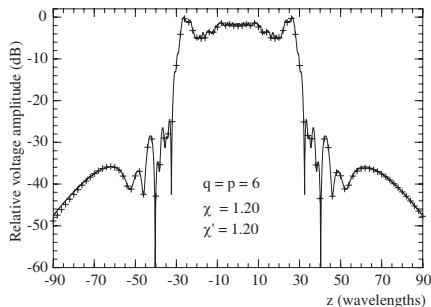


Figure 3. Amplitude of the probe voltage on the generatrix at $\varphi = 90^\circ$. Solid line: exact. Crosses: recovered from irregularly spaced NF helicoidal data via the iterative technique using six iterations.

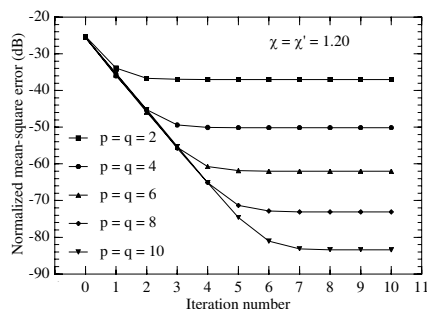


Figure 4. Normalized mean-square errors in the reconstruction of the uniform samples.

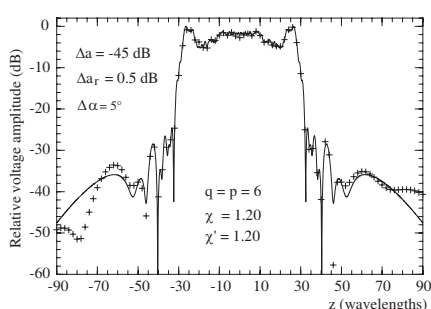


Figure 5. Amplitude of the probe voltage on the generatrix at $\varphi = 90^\circ$. Solid line: exact. Crosses: recovered from irregularly spaced NF helicoidal error affected data via the iterative technique using six iterations.

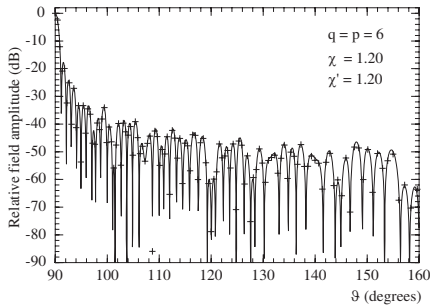


Figure 6. E -plane pattern. Solid line: exact. Crosses: reconstructed from nonuniform NF data.

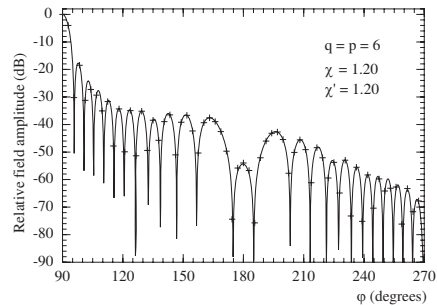


Figure 7. H -plane pattern. Solid line: exact. Crosses: reconstructed from nonuniform NF data.

To provide an overall assessment of the proposed technique, it has been applied to efficiently reconstruct the NF data needed to perform the NF-FF transformation with cylindrical scanning [22]. The resulting FF patterns in the principal planes E and H reconstructed from the nonuniform helicoidal samples are shown in Figs. 6 and 7.

Note that the reconstruction process of the uniform helicoidal samples has taken a CPU time of about 47.7 seconds on a PC equipped with an Intel Core 2 Duo @ 3.33 GHz. Moreover, the number of samples used to recover the NF data on the considered cylinder is 15 153 (guard samples included), significantly less than that (46 080) needed by the standard cylindrical scanning [22] and by the helicoidal scanning technique [23].

The experimental validation of the technique has been carried out in the anechoic chamber available at the laboratory of antenna characterization of the University of Salerno, which is provided with a cylindrical NF facility system supplied by MI Technologies. The probe is an open-ended rectangular waveguide WR90, whose end is tapered for minimizing the diffraction effects. The AUT, located in the plane $x = 0$, is a very simple H -plane monopulse antenna operating at 10 GHz in the sum mode. It has been realized by using two pyramidal horns (8.9×6.8 cm) made by Lectronic Research Labs at a distance of 26 cm (between centers) and a hybrid Tee. According to the sampling representation, the AUT has been modelled as enclosed in a prolate ellipsoid with semi-axes equal to 27 cm and 5 cm. The helix lies on a cylinder with $d = 17.5$ cm and $2h = 240$ cm. In order to assess the effectiveness of the technique in severe conditions as in the case of measurements performed using bad positioners, we have enforced the

acquisition of the NF data in such a way that the distances in ξ and η between the position of each nonuniform sample and the associate uniform one are random variables uniformly distributed in $(-0.3 \Delta\xi, 0.3 \Delta\xi)$ and $(-0.3 \Delta\eta, 0.3 \Delta\eta)$. Note that there was no need to use any optical devices to read the actual sampling positions, since those given by the employed positioners were more than safe.

The amplitude and phase of the probe voltage relevant to the generatrix at $\varphi = 0^\circ$ reconstructed by employing 10 iterations are compared in Figs. 8 and 9 with those directly measured. Note that the phase is shown only in the range $[-20 \text{ cm}, 120 \text{ cm}]$ to improve the readability. As can be seen, in spite of the exaggerated values of the considered positioning errors, there is an excellent agreement between the reconstructed voltage (crosses) and the measured one (solid line), save for the peripheral zone wherein the error is caused both by the truncation of the scanning zone and the environmental reflections. To assess the overall effectiveness of the proposed technique, the FF pattern in the principal planes E and H , reconstructed from the acquired irregularly distributed NF data, is compared in Figs. 10 and 11 with that (reference) obtained from the data directly measured on the classical cylindrical grid. In both the cases, the software package MI-3000 has been used to get the FF reconstructions. Obviously, once the uniform helicoidal data have been retrieved, the OSI algorithm has been employed for recovering the cylindrical data needed to carry out the NF-FF transformation. As can be seen, in both the planes, there is

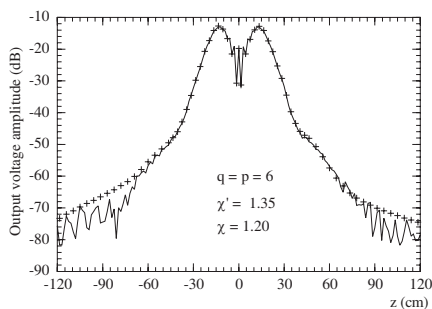


Figure 8. Amplitude of the probe voltage on the generatrix at $\varphi = 0^\circ$. Solid line: measured. Crosses: recovered from irregularly spaced NF data via the iterative approach using ten iterations.

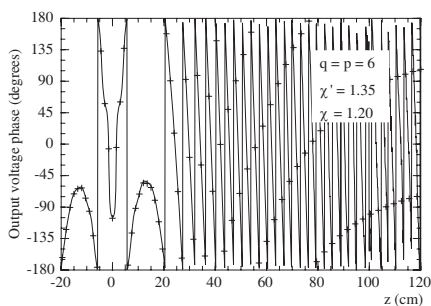


Figure 9. Phase of the probe voltage on the generatrix at $\varphi = 0^\circ$. Solid line: measured. Crosses: recovered from irregularly spaced NF data via the iterative approach using ten iterations.

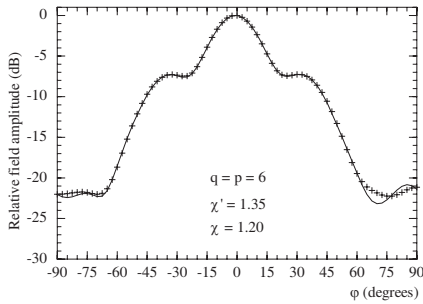


Figure 10. E -plane pattern. Solid line: reference. Crosses: recovered from irregularly spaced NF data via the iterative approach.

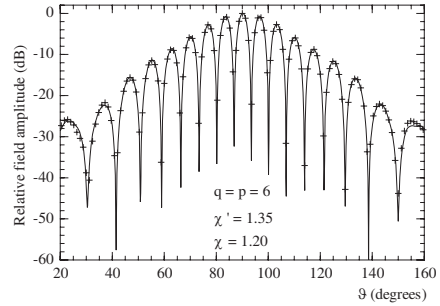


Figure 11. H -plane pattern. Solid line: reference. Crosses: recovered from irregularly spaced NF data via the iterative approach.

a very good agreement, thus assessing the validity of the approach. It is interesting to compare the number of acquired nonuniform NF data (1 620) with that (5 760) required to cover the same measurement zone by the standard NF cylindrical scanning and the half wavelength helicoidal scanning technique [23].

REFERENCES

1. Bolomey, J. C., et al., "Rapid near-field antenna testing via array of modulated scattering probes," *IEEE Trans. Antennas Propagat.*, Vol. 36, 804–814, June 1988.
2. Yaccarino, R. G., L. I. Williams, and Y. Rahmat-Samii, "Linear spiral sampling for the bipolar planar antenna measurement technique," *IEEE Trans. Antennas Propagat.*, Vol. 44, 1049–1051, 1996.
3. Bucci, O. M., C. Gennarelli, G. Riccio, and C. Savarese, "Nonredundant NF-FF transformation with helicoidal scanning," *Journal of Electromagnetic Waves and Applications*, Vol. 15, No. 11, 1507–1519, 2001.
4. Bucci, O. M., F. D'Agostino, C. Gennarelli, G. Riccio, and C. Savarese, "Probe compensated FF reconstruction by NF planar spiral scanning," *IEE Proc. — Microw. Ant. Prop.*, Vol. 149, 119–123, April 2002.
5. Bucci, O. M., F. D'Agostino, C. Gennarelli, G. Riccio, and C. Savarese, "NF-FF transformation with spherical spiral

- scanning,” *IEEE Antennas Wireless Propagat. Lett.*, Vol. 2, 263–266, 2003.
6. D’Agostino, F., C. Gennarelli, G. Riccio, and C. Savarese, “Theoretical foundations of near-field-far-field transformations with spiral scanings,” *Progress In Electromagnetics Research*, Vol. 61, 193–214, 2006.
 7. D’Agostino, F., F. Ferrara, C. Gennarelli, R. Guerriero, and M. Migliozzi, “Near-field-far-field transformation technique with helicoidal scanning for elongated antennas,” *Progress In Electromagnetics Research B*, Vol. 4, 249–261, 2008.
 8. D’Agostino, F., F. Ferrara, C. Gennarelli, R. Guerriero, and M. Migliozzi, “An effective NF-FF transformation technique with planar spiral scanning tailored for quasi-planar antennas,” *IEEE Trans. Antennas Propagat.*, Vol. 56, 2981–2987, September 2008.
 9. D’Agostino, F., F. Ferrara, C. Gennarelli, R. Guerriero, M. Migliozzi, and G. Riccio, “A nonredundant near-field to far-field transformation with spherical spiral scanning for nonspherical antennas,” *The Open Electr. & Electronic Engin. J.*, Vol. 3, 1–8, 2009.
 10. D’Agostino, F., F. Ferrara, J. A. Fordham, C. Gennarelli, R. Guerriero, M. Migliozzi, G. Riccio, and C. Rizzo, “An effective NF-FF transformation technique for elongated antennas using a fast helicoidal scan,” *IEEE Antennas Propagat. Magaz.*, Vol. 51, 134–141, 2009.
 11. D’Agostino, F., F. Ferrara, C. Gennarelli, R. Guerriero, and M. Migliozzi, “Laboratory tests assessing the effectiveness of the NF-FF transformation with helicoidal scanning for electrically long antennas,” *Progress In Electromagnetics Research*, Vol. 98, 375–388, 2009.
 12. D’Agostino, F., F. Ferrara, C. Gennarelli, R. Guerriero, and M. Migliozzi, “The unified theory of near-field-far-field transformations with spiral scanings for nonspherical antennas,” *Progress In Electromagnetics Research B*, Vol. 14, 449–477, 2009.
 13. Bucci, O. M., C. Gennarelli, and C. Savarese, “Representation of electromagnetic fields over arbitrary surfaces by a finite and nonredundant number of samples,” *IEEE Trans. Antennas Propagat.*, Vol. 46, 351–359, March 1998.
 14. Dutt, A. and V. Rohklin, “Fast Fourier transforms for nonequispaced data,” *Proc. of SIAM J. Scie. Comput.*, Vol. 14, 1369–1393, November 1993.
 15. Beylkin, G., “On the fast Fourier transform of functions with singularities,” *Appl. Comput. Harmonic Anal.*, Vol. 2, 363–381,

- 1995.
16. Wittmann, R. C., B. K. Alpert, and M. H. Francis, "Near-field antenna measurements using nonideal measurement locations," *IEEE Trans. Antennas Propagat.*, Vol. 46, 716–722, May 1998.
 17. Wittmann, R. C., B. K. Alpert, and M. H. Francis, "Near-field, spherical scanning antenna measurements with nonideal probe locations," *IEEE Trans. Antennas Propagat.*, Vol. 52, 2184–2186, August 2004.
 18. Bucci, O. M., C. Gennarelli, and C. Savarese, "Interpolation of electromagnetic radiated fields over a plane from nonuniform samples," *IEEE Trans. Antennas Propagat.*, Vol. 41, 1501–1508, November 1993.
 19. Bucci, O. M., C. Gennarelli, G. Riccio, and C. Savarese, "Electromagnetic fields interpolation from nonuniform samples over spherical and cylindrical surfaces," *IEE Proc. Microw. Antennas Propagat.*, Vol. 141, 77–84, April 1994.
 20. Ferrara, F., C. Gennarelli, G. Riccio, and C. Savarese, "NF-FF transformation with cylindrical scanning from nonuniformly distributed data," *Microw. Optical Tech. Lett.*, Vol. 39, 4–8, October 2003.
 21. D'Agostino, F., F. Ferrara, C. Gennarelli, R. Guerriero, and M. Migliozzi, "On the compensation of probe positioning errors when using a nonredundant cylindrical NF-FF transformation," *Progress In Electromagnetics Research B*, Vol. 20, 321–335, 2010.
 22. Leach, W. M., Jr. and D. T. Paris, "Probe compensated near-field measurements on a cylinder," *IEEE Trans. Antennas Propagat.*, Vol. 21, 435–445, July 1973.
 23. Costanzo, S. and G. Di Massa, "Far-field reconstruction from phaseless near-field data on a cylindrical helix," *Journal of Electromagnetic Waves and Applications*, Vol. 18, No. 8, 1057–1071, 2004.